Int. J. Thermodynamics, **ISSN 1301-9724**
Vol. 7, (No. 3), pp.141-148, September-2004

Effect of the Structured Packing on Column Diameter, Pressure Drop and Height in a Mass Transfer Unit

Rosa H. Chávez
Gerencia de Ciencias Ambientales, Instituto Nacional de Investigaciones Nucleares
km. 36.5 Carretera México – Toluca, Municipio de Ocoyoacac 52045
Salazar Estado de México, MEXICO,
Tel +(52)-5553297200 ext.2649, Fax +(52)-5553297301
E-mail: rhch@nuclear.inin.mx

Javier de J. Guadarrama
Departamento de Ingeniería Eléctrica y Electrónica
Instituto Tecnológico de Toluca, MEXICO
E-mail:jguad4@aol.com

Abel Hernández-Guerrero
Department of Mechanical Engineering, Universidad de Guanajuato,
Apartado Postal 215A, Tampico 912, Salamanca, Gto., 36730, MEXICO,
E-mail:abelh@salamanca.ugto.mx

Abstract

In order to determine the dimension of a separation column, hydrodynamic and mass transfer models are necessary to evaluate the pressure drop and the mass transfer unit height. The present work evaluates the dependency of those parameters with respect to the diameter of the column by means of an absorption column. The process within the absorption column is carried out using three different structured-packings (ININ, Sulzer BX, and Mellapak) and one hazardous packing (Raschig rings), in order to recover SO_2. Structured packing has been achieving wider acceptance due to its greater efficiency in the separation process. The results show how the ININ packing does the best work because it has the lowest height of the global mass transfer unit and the Mellapak packing has the largest capacity because it manages the largest flows.

Keywords: Structured Packing, Mass Transfer Unit, Absorption Column

1. Introduction

Mass transfer and hydrodynamic models for packed mass transfer column units are developed based on gross measurements representative of the entire length of the contacting column. These measurements include overall column pressure drop, as an indication of the hydraulic behavior of the packing, and concentration changes as an indication of the mass transfer efficiency of the specific column intervals being studied. While this approach has served the chemical processing industry relatively well, it falls significantly short in its ability to provide a fundamental understanding of the internal flow behavior (Chavez et al., 1999, Schmit et al., 2001.)

In a wet method, an exhaust gas is introduced into an aqueous alkali sulfite solution to induce the reaction of the sulfur dioxide contained in the aqueous exhaust gas with the alkali sulfite to obtain the alkali mono-hydrogen-sulfite solution (alkali bisulfite). The reaction mechanism in the method can be expressed by the following reaction where sodium sulfite is used as an alkali sulfite (Patent US3989796):

$$SO_2 + Na_2SO_3 + H_2O \Leftrightarrow 2NaHSO_3$$

The main purpose of the present paper is to evaluate the dependency of both the pressure drop and the height of the global mass transfer unit with respect to the diameter of the column, using an absorption conventional method, adapting columns with high-efficiency structured packings like ININ, Sulzer BX, and Mellapak packings and also with one hazardous packing

(Raschig rings), and using hydrodynamic and mass transfer models in order to design columns.

The ideal and expected modus operandi of a gas-liquid contactor is one in which the continuous phase is the gas and the dispersed phase is the absorbing liquid. If flow rate and other conditions are such that the liquid phase becomes continuous and the gas phase becomes dispersed, then we have the very inefficient and unpredictable condition called flooding. For the general case of mass transfer between two phases, concentration gradients can exist on each side of the interface. If the two phases are in turbulent flow or in the loading zone, the concentration gradients may be significant only in the effective films (laminar sublayer or stagnant regions) on each side of the interface. Thus, these films limit the total mass transfer process (Stichlmair et al., 1989; Rocha et al., 1996).

2. Materials and Methods

The methodology was divided in two parts: i) model simulation (hydrodynamic and mass transfer models used to determine the hydrodynamic behavior and mass transfer efficiency of the column), and ii) the use of different packings to compare the column dimensions and the operating conditions resulting from its use.

2.1 Hydrodynamic model structured packings

The pressure drop model (Stichlmair et al., 1989) has been used for the prediction of pressure drop and flooding in packed columns. The gas and liquid are flowing in a countercurrent fashion. A mathematical expression to describe all flow regimes (dry gas, irrigated gas flow below the load point, loading region, and flooding region), for any kind of packing materials, is as follows:

$$\frac{\Delta P_{irr}}{r_L g Z} = \frac{\Delta P_{dry}}{r_L g Z} AB \qquad (1)$$

$$A = \frac{1}{1-\varepsilon}\left\{1-\varepsilon\left[1-\frac{h_0}{\varepsilon}\left[1+20\left(\frac{\Delta P_{irr}}{r_L g Z}\right)^2\right]\right]\right\}^{(2+c)/3} \qquad (2)$$

$$B = \left[1-\frac{h_o}{\varepsilon}\left[1+20\left(\frac{\Delta P_{irr}}{r_L g Z}\right)^2\right]\right]^{-4.65} \qquad (3)$$

Where ΔP_{irr}, is the irrigated pressure drop (Pa/m), ΔP_{dry} is the dry pressure drop (Pa/m), ρ_G, ρ_L are the gas and liquid densities (kg/m^3), respectively, g is the gravitational acceleration (m/s^2), Z is the column height (m), ε is the porosity of the packing (m^3/m^3), h_0 is the liquid hold up in the load point (m^3/m^3) and c is an exponent given by:

$$c = \frac{1}{f_o}\left(-\frac{c_1}{Re_G}-\frac{c_2}{2\sqrt{Re_G}}\right) \qquad (4)$$

The friction factor for a single particle is:

$$f_o = \frac{c_1}{Re_G}+\frac{c_2}{\sqrt{Re_G}}+c_3 \qquad (5)$$

where c_1 c_2 and $c_3$are the fitting parameters, and Re_G is the Reynolds number of the gas flow.

The force acting on the liquid to move it downward through the packing is gravity. Several forces oppose gravity: (a) liquid buoyancy (important at high pressures), (b) vapor pressure drop, and (c) drag on the liquid film by the vapor. On the basis of data analysis for the sake of simplicity, as well as to maintain positive values of g_{eff} at all times as a result of the equilibrium of forces, a value of 1025 Pa/m was selected for the flooding pressure drop.

$$g_{eff} = g\left[\left(\frac{\rho_L-\rho_G}{\rho_L}\right)\left(1-\frac{\Delta P/\Delta Z}{1025}\right)\right] \qquad (6)$$

The pressure drop is calculated iteratively in the loading region, near the 1025 Pa/m criterion, or up to 90 % flooding, using equation (1).

In order to determine c_1, c_2 and c_3 the *Levenberg-Marquardt Method* is used (More, 1978) and the experimental pressure drop data. Initially the values for c_1, c_2 and c_3 are assumed, and then when the sum of squares of the differences (i.e. the experimental values minus the theoretical values) reach a minimum or they are less than or equal to the convergence parameter, c_1, c_2 and c_3 are obtained. TABLE I shows the experimental pressure drop data (ΔP in Pa/m) obtained using a 1.7 m height absorption column, and packed with ININ packing, with an air-water system, at 25 ºC and 760 mm Hg as the operation conditions. The gas flow (F_{SE} in m/s(kg/m^3)$^{1/2}$) is expressed by the product of the gas velocity plus the square root of the gas density. TABLE II shows the fitting parameters from the pressure drop model (Stichlmair et al., 1989).

The standard deviation σ is considered to give a fairly accurate picture of data variation for a single set of measurements. The mean of all responses in a population will be indicated by the symbol y. For an approximately normal distribution of measurements (bell shaped), it follows that the interval with endpoints: y $\pm\sigma$ contain approximately 68% of the measurements,

y±2σ contain approximately 95% of the measurements, and y±3σ contain almost all of the measurements (Chávez, 2004b).

TABLE I. EXPERIMENTAL PRESSURE DROP DATA ΔP AT DIFFERENT GAS FLOW F_{SE} AND DIFFERENT LIQUID FLOW U_L.

$F_{SE}\rightarrow$	0.047	0.071	0.09	0.13	0.14	0.17
$U_L\downarrow$						
0.0	5.60	8.6	11.4	14.2	17.1	20.0
0.061	6.95	11.4	15.7	21.0	26.5	32.4
0.109	10.5	17.1	23.1	29.9	38.0	46.5
0.132	14.5	22.1	31.8	40.4	51.9	65.3
0.156	19.2	29.9	42.9	57.9	73.6	90.0
0.180	24.0	40.4	60.0	84.4	109.	160.
0.19	28.7	49.4	75.9	105.	170.	300.

TABLE II. FITTING PARAMETERS AT DIFFERENT U_L.

U_L	C_1	C_2	C_3	y±2σ
0.0616	0.8321	1.0472	0.1718	95.93%
0.1090	3.9031	–0.5515	0.8735	96.56%
0.1326	4.2575	–0.6250	1.1959	95.92%
0.1563	4.7524	–0.2973	1.2501	95.92%
0.1800	0.8666	0.6419	1.1363	93.77%
0.1918	–0.1971	1.7958	2.1441	76.85%
Mean→	2.40245	0.33519	1.07137	

2.2 Mass transfer model for structured packings

The *Two-Resistance Model* (Rocha et al., 1996) is used, with the assuming thermodynamic equilibrium at the phases interface. This assumption applies only to structured packings in the loading region. The basic parameters of the model are the gas (or vapor) phase mass transfer coefficient, the liquid phase coefficient, and the effective interfacial area.

$$\left(\frac{K_G\, s}{D_G}\right) = 0.054\left[\frac{\left(U_{L,eff}+U_{G,eff}\right)\rho_G\, s}{\mu_G}\right]^{0.8}\left(\frac{\mu_G}{D_G\ \rho_G}\right)^{0.33} \quad (7)$$

$$K_L = \sqrt{\frac{D_L\ U_{L,eff}}{\pi\ s C_E}} \quad (8)$$

$$\frac{a_e}{a} = F_{SE}\ \left[\frac{29.12\ \left(We_L\ Fr_L\right)^{0.15}\ s^{0.359}}{Re_L^{0.2}\varepsilon^{0.6}\ \left(1-Cos\gamma\right)\ \left(Sen\theta\right)^{0.3}}\right] \quad (9)$$

In this model, K_G, K_L are the mass transfer coefficients of the gas and liquid phase, respectively; a is the geometric packing area per volume packed unit (m^2/m^3); a_e is the effective interfacial area per volume unit (m^2/m^3); the product of $K_G\ a_e$, $K_L\ a_e$ are the mass transfer volumetric coefficients of the gas and liquid phase, respectively, per unit time in hours (1/h); s is the corrugated side of the structured packings (m); D_L, D_G are the solute diffusivities of liquid and gas phase, respectively (m^2/s); μ_L, μ_G are the viscosities of the liquid and gas, respectively (kg/(ms)); $U_{G,eff}$, $U_{L,eff}$ are the effective velocities of gas and liquid, respectively (m/s); C_E is the correction factor for surface renewal equal to 0.9; F_{SE} is a factor for surface enhancement equal to 0.26; Fr_L is the Froude number of liquid flow; Re_L is the Reynolds number of the liquid flow; We_L is the Weber number of the liquid flow; γ is the contact angle between solid and liquid film; and θ is the corrugated angle of the structured packing.

On the basis of conventional definitions of transfer units, the height of a gas phase transfer unit is:

$$HTU_G = \frac{U_G}{K_G a_e \rho_G} \quad (10)$$

And the height of a liquid phase transfer unit is:

$$HTU_L = \frac{U_L}{K_L a_e \rho_L} \quad (11)$$

where U_G and U_L are the velocities of the gas and liquid flows (m/s), respectively.

The application of the Two-Film Model is frequently used to relate the height of the global mass transfer unit HTU_{OG}, HTU_{OL} with the height of the gas HTU_G and liquid HTU_L mass transfer units. The heights of the global mass transfer units are determined as follows:

On the gas-side:

$$HTU_{OG} = HTU_G + \lambda HTU_L \quad (12)$$

And on the liquid-side:

$$HTU_{OL} = HTU_L + \frac{1}{\lambda} HTU_G \quad (13)$$

The Two- Film Model is based on the number of global mass transfer units, NTU_{OG} and NTU_{OL}, of both gas and liquid resistance, and it involves the efficiency in terms of the height of a global mass transfer unit HTU_{OG}, HTU_{OL} (Chávez and Guadarrama, 2004a, Xu et al., 2000).

On the gas phase side the column height

$$Z = HTU_{OG} \cdot NTU_{OG} \quad (14)$$

And on the liquid phase side the column height

$$Z = HTU_{OL} \cdot NTU_{OL} \quad (15)$$

In a generalized situation, if the gas is highly soluble in the liquid, the Henry constant will be small. In this case the liquid side resistance is negligible. If the gas is relatively insoluble (large value of the Henry constant), the gas side resistance becomes negligible in comparison with the liquid side resistance. The relative magnitude of the individual resistance evidently depends on the gas solubility, as represented by the Henry's law constant. This explains the common statements that "the liquid side resistance is controlling" in the absorption of a relatively insoluble gas, and the "gas side resistance is controlling" when a relatively soluble gas is absorbed (or stripped).

$$\lambda = m\frac{U_G}{U_L} \quad (16)$$

Here the parameter λ is the ratio of the equilibrium line slope to the operating line slope, and λ is known as the removal factor. The inverse of λ is known as the absorption factor, and m is the ratio of Henry´s law constant to atmospheric pressure and 25 ºC equal to 0.36.

TABLE III. GEOMETRIC CHARACTERISTICS OF DIFFERENT STRUCTURED PACKINGS.

Packing	ε (m^3m^{-3})	θ (º)	a (m^2/m^3)	γ (º)
ININ	0.98	45	1033	45
SulzerBX	0.96	60	450	30
Mellapak	0.85	45	350	45
Raschig	0.75	Does not apply	274	Does not apply

TABLE IV. FEED LIQUID FLOW CONDITION AT THE TOP OF THE COLUMN (PATENTUS3989796).

Compounds	Mol percent	Molecular weight kg/kgmol	Mass flow kg/h	Molar flow kgmol/h	Weight percent
Na_2SO_3	2.39	126.05	120.82	0.96	14.0
Na_2SO_4	0.75	142.05	43.15	0.30	5.0
H_2O	96.85	18.00	699.03	38.83	81.0
Total	100.00	Not necessary	863.00	40.09	100.0

TABLE V. EXIT LIQUID FLOW CONDITION AT THE BOTTOM OF THE COLUMN, 889 KG/H (PATENT US3989796).

Compounds	Mol percent	Molecular weight kg/kgmol	Mass flow kg/h	Molar flow kgmol/h	Weight percent
$NaHSO_3$	1.52	104.06	64.01	0.61	7.2
Na_2SO_3	1.62	126.05	82.05	0.65	9.2
Na_2SO_4	0.75	142.05	43.27	0.30	4.9
H_2O	96.11	18.00	699.64	38.87	78.7
Total	100.00	Not necessary	888.97	40.43	100.0

TABLE VI. FEED GAS FLOW CONDITION AT THE BOTTOM OF THE COLUMN (PATENTUS3989796).

Compounds	Mol percent	Molecular weight kg/kgmol	Volumetric flow (m^3/h)	Molar flow kgmol/h	Mass flow kg/h
SO_2	0.14	64	7.03	0.31	20.07
Air	99.86	24	4992.97	222.76	6460.04
Total	100.00	Not necessary	5000.00	223.07	6480.11

TABLE VII. EXIT GAS FLOW CONDITION AT THE TOP OF THE COLUMN (PATENT US3989796).

Compounds	Mol percent	Molecular weight kg/kgmol	Volumetric flow (m^3/h)	Molar flow kgmol/h	Mass flow kg/h
SO_2	0.0028	64	0.14	0.0062	0.39
Air	99.9972	24	4992.96	222.7611	6460.72
Total	100.0000	Not necessary	4993.10	222.7673	6461.11

TABLE VIII. IRRIGATED PRESSURE DROP AND GLOBAL MASS TRANSFER UNIT HEIGHT RESULTS, EVALUATED FROM THE HYDRODYNAMIC AND MASS TRANSFER MODELS.

Packing	**a** (m^2)	ϕ (m)	U_G (m/s)	U_L (m/s)	ΔP_{irr} (Pa/m)	HTU_{OL} (m)	Z (m)	%Floodin
Sulzer BX	1.76	1.499	0.927	1.60E-04	137.55	5.83	61.83	13.42
	1	1,128	1,23	2.12E-04	320.18	3.81	40.44	31.24
	0.75	0,977	1,421	2.45E-04	506.67	2.84	30.15	49.43
	0.65	0,909	1,526	2.63E-04	642.57	2.30	24.40	62.69
	0.55	0,836	1,659	2.86E-04	857.08	1.46	15.48	83.61
	0.51	0,805	1,723	2.97E-04	981.29	0.76	8.11	95.74
	0.5	0,797	1,740	3.00E-04	1017.44	0.33	3.56	99.26
ININ	1.76	1.496	0.927	1.60E-04	329.42	1.87	19.88	32.14
	1	1.128	1.230	2.12E-04	894.49	0.61	6.53	87.27
	0.95	1.099	1.262	2.18E-04	988.29	0.32	3.43	96.42
	0.94	1.094	1.269	2.19E-04	1009.17	0.21	2.23	98.46
Mellapak	1.76	1.496	0.927	1.60E-04	57.44	5.98	63.34	5.60
	1.	1.128	1.230	2.12E-04	142.70	4.22	44.79	13.92
	0.3999	0.713	1.946	3.36E-04	715.95	1.71	18.18	69.84
	0.3499	0.667	2.080	3.59E-04	930.23	0.96	10.24	90.75
	0.3399	0.657	2.111	3.64E-04	986.72	0.64	6.78	96.26
	0.3350	0.653	2.126	3.67E-04	1017.29	0.30	3.22	99.25
Raschig	1.7600	1.497	0.789	1.36E-04	393.09	6.66	70.58	38.35
	1.200	1.236	1.157	1.99E-04	817.58	3.26	34.55	79.76
	1.100	1.183	1.262	2.18E-04	971.48	1.68	17.89	94.77
	1.0750	1.169	1.291	2.23E-04	1017.35	0.69	7.30	99.25

2.3 Use of different packings and different liquid and gas flow condition

TABLE III shows the geometric characteristics of the different structured packings: ININ, Sulzer BX, Mellapak and Raschig rings used in this work. TABLEs IV, V, VI and VII show the liquid and gas flow conditions. *Figures* 5 and 6 show corrugated gauze of metal and ININ structured packing, respectively.

3. Results

TABLE VIII shows the irrigated pressure drop ΔP_{irr} and the global mass transfer unit height HTU_{OL} evaluated by the hydrodynamic and mass transfer models, respectively. The iteration was stopped when the flooding percent reached the largest value (between 98.46 and 99.26% flooding), assuring the process to be in the loading regime or turbulent flow. It was considered that the flooding section was reached when the pressure drop was on the order of 1025 Pa/m (Rocha et al., 1996).

Figures 1 and *2* show that the Mellapak packing has the largest capacity with the lowest diameter because it handles the largest gas and liquid flows in the column. The Sulzer BX packing came second, then the ININ packing and finally the Raschig rings. All of the packings were operated in the loading region, near the flooding zone (1025 Pa/m), up to 90% flooding.

Figure 3 shows the irrigated pressure drop with respect to the diameter of the column. The smallest cross section, for all packings, was present in the loading regime, near the flooding zone. The figure shows that the largest irrigated pressure drop was for the Raschig rings, then came the ININ, followed by the Sulzer BX and finally by the Mellapak packing. This result is due to the porosity and the number of strings with which they are built, with respect to structured packing. The ININ packing has 16 strings, the Sulzer BX packing has 10, and the Mellapak has 6.

Figure 4 shows the height of the global mass transfer unit versus the diameter of the column; the largest efficiency is seen again in the loading regime, near the flooding zone. The figure shows that the ININ packing was more efficient than the Sulzer BX packing, mainly due to the fact that the height of the mass transfer global unit for the ININ packing proved to be the smallest height, as compared to the heights of the units when the Raschig rings or the Sulzer BX or Mellapak packings were used.

For the sake of better understanding the geometry of the structured packings, at the end of this paper, pictures of the ININ packing are shown (Figures 5 and 6).

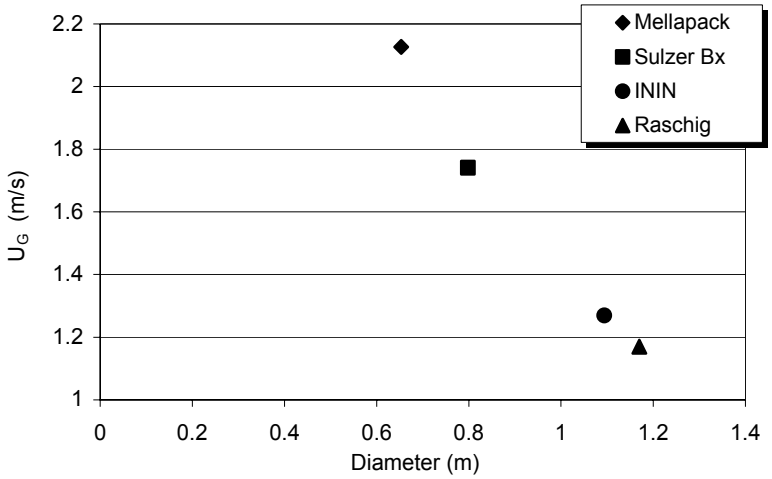

Figure 1. Gas velocities versus the diameter of the column, between 98.46 and 99.26% flooding.

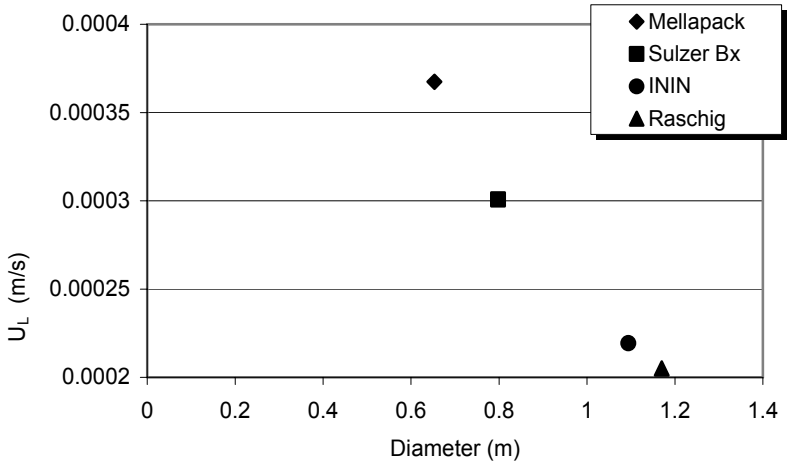

Figure 2. Liquid velocity versus the diameter of the column, between 98.46 and 99.26% flooding.

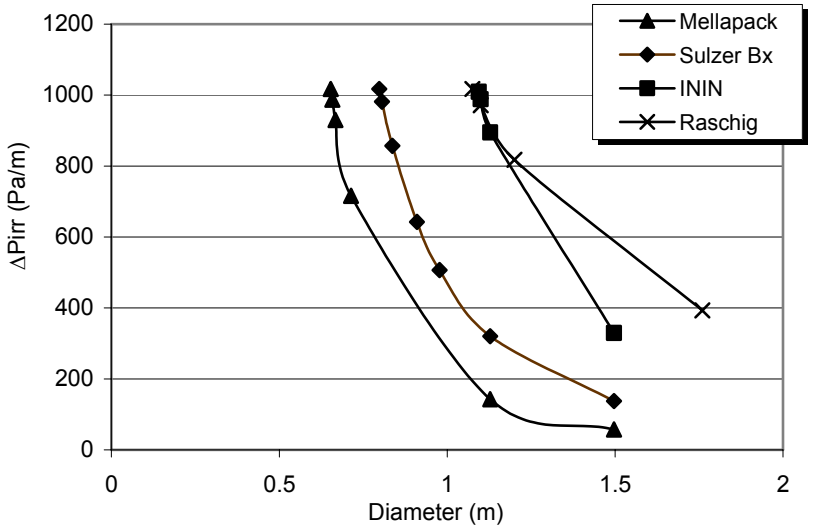

Figure 3. Irrigated pressure drop versus the diameter of the column, between 5.6 and 99.26% flooding.

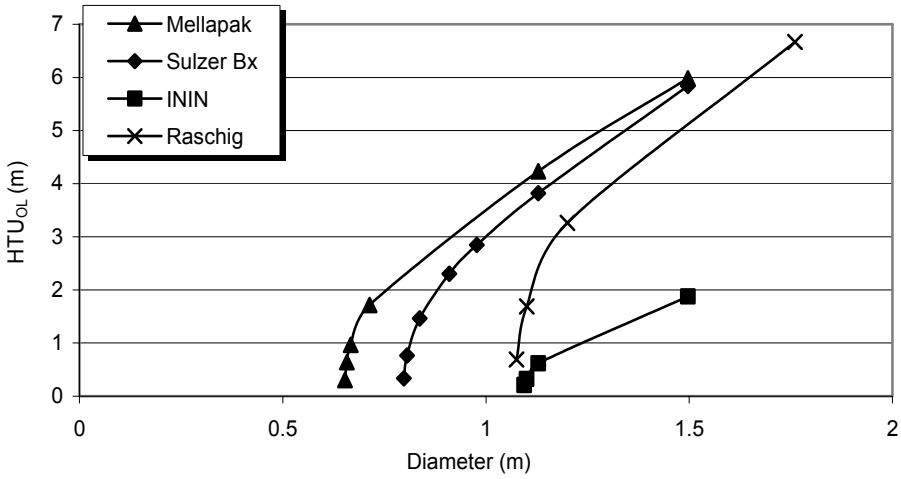

Figure 4. Mass transfer unit height versus the diameter of the column, between 5.6 and 99.26% flooding.

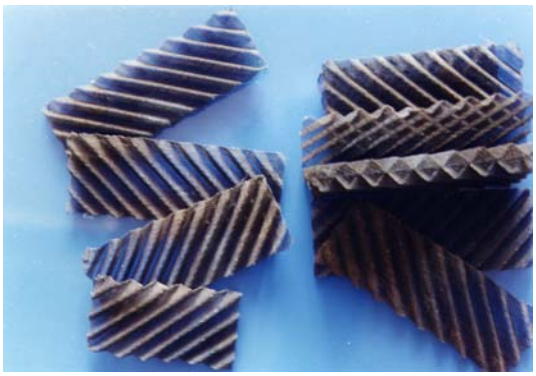

Figure 5. Corrugated gauze of metal.

Figure 6. View of the ININ structured packing.

4. Conclusions

The methodology discussed in this paper shows that the diameter of the column is an important parameter in the design of packed columns. This is because of the strong dependence of the pressure drop and the height of the global mass transfer unit to the diameter of the column.

The influence of the diameter of the column in the evaluation of hydrodynamic and mass transfer parameters differs for the four structured packings studied. This is due to their different geometric characteristics, despite operating at a similar load regime value.

The methodology presented here also enables the finding of the best operating condition for the column, as well as determining the sizes required to achieve the best response without being in the flooding zone. This is because it enables one to simulate in regions very close to flooding and to evaluate the diameter of the column, the pressure drop, and the global height of the mass transfer unit.

The impact on revamping structured packing in lieu of hazardous packing in a separation column would enable one to manage higher flows and higher separation efficiency.

Acknowledgement

Financial support of this work was provided by Consejo Nacional de Ciencia y Tecnología (CONACYT), project: I36297U.

Nomenclature

A	Cross sectional area of the column, m^2
a	Geometric packing area per volume packed unit, m^2/m^3
a_e	Effective interfacial area per volume unit, m^2/m^3
c_1, c_2, c_3,	Fitting parameters
C_E	Correction factor for surface renewal, equal to 0.9
D_G	Solute diffusivity of gas phase, m^2/s
D_L	Solute diffusivity of liquid phase, m^2/s
Fr_L	Froude number of liquid flow

F_{SE}	Factor for surface enhancement,equal to 0.26
g	Gravitational constant, m/s^2
h_0	Liquid hold up at load point m^3/m^3
HTU_G	Height of the gas mass transfer units, m
HTU_l	Height of the liquid mass transfer units, m
HTU_{OG}	Global height of the gas mass transfer units, m
HTU_{OL}	Global height of the liquid mass transfer units, m
$K_G\ a_e$	Mass transfer volumetric coefficient of the gas phase, 1/h
$K_L\ a_e$	Mass transfer volumetric coefficient of the liquid phase, 1/h
m	Ratio of Henry´s law constant to atmospheric pressure
NTU_{OG}	Number of mass transfer global units of both gas resistances
NTU_{OL}	Number of mass transfer global units of liquid resistances
Re_G	Reynolds number of gas flow
Re_G	Reynolds number of liquid flow
s	Corrugated side of the structured packings, m
U_G	Gas velocities, m/s
U_L	Liquid velocities, m/s
$U_{G,eff}$	Effective velocity of gas, m/s
$U_{L,eff}$	Effective velocity of liquid, m/s
We_L	Weber number of liquid flow
Z	Column height, m

Greek

ΔP_{dry}	Dry pressure drop, Pa/m
ΔP_{irr}	Irrigated pressure drop, Pa/m
ε	Porosity of the packing, m^3/m^3
γ	Contact angle between solid and liquid film,º
ϕ	Diameter of the column, m
λ	Ratio of the equilibrium line slope to the operating line slope
μ_G	Viscosity of the gas, kg/(ms)
μ_L	Viscosity of the liquid, kg/(ms)
$_,\rho G$	Gas density, kg/m^3
ρL	Liquid density, kg/m^3
θ	Corrugated angle of the structured packing

References

Chávez T.R.H., Suástegui R.A.O., and Guadarrama G.J.J., 1999, "Evaluación de la Altura Equivalente por Plato Teórico a un Empaque Estructurado Nacional", *Revista Internacional Información Tecnológica Chilena* (ISSN: 0716-8576), V2, No.2, pp. 81-86, Marzo-Abril.

Chávez T.R.H. and Guadarrama G.J.J., 2004a, "Caracterización Experimental de un Empaque Estructurado de Gasa de Latón", *Revista Internacional Información Tecnológica Chilena* (ISSN: 0716-8576), V15, No.1, pp.17-22.

Chávez R.H. and Guadarrama J.J., 2004b, "Ajuste de un Modelo Hidrodinámico para una Columna con Empaques Estructurados usando Valores Experimentales", *Información Tecnológica - Revista Internacional* – La Serena – Chile, V15, No.2, pp.19-24.

More, J.J., 1978, "The Levenberg-Marquardt Algorithm: Implementation and Theory", In Numerical Analysis – *Proceedings Dundee*, *Lecture Notes in Mathematics*, v630, Spring – Verlag, pp.105-116.

Pat. US3989796 (Nov. 2, 1976), Morita Tomijiro, Funahashi Isao, Igarashi Koichi and Takaiwa Masakazu, "Method for Removing Sulfur Dioxide in the Form of Calcium from Combustion Exhaust Gas."

Rocha J.A., Bravo J.L. and Fair J.R., 1996, "Destillation Columns Containing Structured Packing, a Comprehensive Model for their Performance. Mass Transfer Model", *Industrial* Engineering Chemistry Research, V35, No.5, pp. 1660-1667.

Schmit C.E., Cartmel D. B. and Bruce Eldridge, 2001, "The Experimental Application of X-ray Tomography to a Vapor-Liquid Contactor", *Chemical Engineering Science*, 56, pp. 3431-3441.

Stichlmair J.J., Bravo J.L., Fair J.R., 1989, "General Model for Prediction of Pressure Drop and Capacity of Counter Current Gas/Liquid Packed Columns", *Gas Separation & Purification* V3, March, pp. 19-28.

Xu, Z.P., Afacan A., Chuang K.T., 2000, "Predicting Mass Transfer in Packed Columns Containing Structured Packings", Chemical Engineering Research and Design, *Transactions of the Institute of Chemical Engineers*, Part A V78, No.1, pp. 91-98.